Advances in Machinery, Materials Science and Engineering Application
M. Chen et al. (Eds.)

doi:10.3233/ATDE220482

Evolution of Microstructure and Mechanical Properties of the Gears on Coal-Cutting Machines in the Processes of Rapid Carburization and Heat Treatments: Numerical Modeling and Experiments

Yuedong YUAN [a,1], Qingyu ZHANG [a,b,2], Yu XUE [a], Xinjun SHEN [b], Yang JIANG [b], Kun LIU [a] and Xiaonan WANG [a,b]
[a] *Changshu Tiandi Coal Machinery Equipment Co., Ltd., Suzhou, 215500, China*
[b] *School of Iron and Steel, Soochow University, Suzhou, 215137, China*

Abstract. To modify the rapid carburization and heat treatments of 18Cr2Ni4WA heavy-duty gears on coal-cutting machines, numerical modeling and experimental investigations are carried out for understanding the evolution of microstructure and properties. Through numerical modeling, the fractions of austenite, bainite, and martensite are evaluated. The Vickers hardness distribution across the hardening layer, calculated by the Maynier equation, compares well with the experimental measurement. The microstructure of the hardening layer is mainly composed of fine martensite and carbides, while that of the interior area is the martensite. The gradient of the microstructure from the hardening layer to the interior area leads to the variation of the hardness distribution. The experimental results show that the high-temperature tempering and quenching are beneficial for the refinements of the grains in the hardening layer and the interior area. The present study indicates that the combination of numerical modeling and experimental observation provides a powerful tool for the modification and improvement of the carburization and heat treatment processes.

Keywords. Rapid carburization, heat treatment, microstructure, alloy steel, numerical modeling

1. Introduction

The coal-cutting machine is one of the most important heavy types of machinery in the coal industry. The fabrication of heavy-duty gears on the coal-cutting machines receives consistent interest from heat treatment engineers, since the mechanical properties of the heavy-duty gears, e.g. hardness, wear resistance, and toughness, are significant to the long-term performances of coal-cutting machines [1]. In the process of gear engagement,

[1] Yuedong Yuan, Corresponding author, Changshu Tiandi Coal Machinery Equipment Co., Ltd., Suzhou, 215500, China; E-mail: csyyd@126.com.
[2] Qingyu Zhang, Corresponding author, Changshu Tiandi Coal Machinery Equipment Co., Ltd., Suzhou, 215500, China; School of Iron and Steel, Soochow University, Suzhou, 215137, China; E-mail: qingyu.zhang@suda.edu.cn.

there are not only rolling motions, but also sliding frictions, which produce pulsation cycles of stress on the tooth surfaces. Thus, it is extremely important to strengthen the tooth surfaces in a large case depth [2]. The heavy-duty gears are usually fabricated by using alloy steels. In general, the tooth surfaces of these gears can be hardened and strengthened through carburization heat treatments, and the heat treatment quality can determine the mechanical properties and the service performance drastically [3, 4]. For domestic coal-cutting equipment, the alloy steels for producing the gears in the travel units are 18Cr2Ni4WA and 20Cr2Ni4, which can exhibit high wear resistance and anti-fatigue performance after the carburization heat treatments. However, the carburization time could exceed 150 hours for obtaining a 4 mm thick effective hardening layer under the carburization temperature of c.a. 920 ℃, which greatly reduces the production efficiency.

To increase the carburization efficiency, it is required to increase the carburization temperature, and the subsequent heat treatments should be modified accordingly. In the traditional R&D routine, many trial-and-error experiments should be performed to modify the parameters in the carburization and heat treatment techniques [5, 6]. However, the efficiency of the trial-and-error experiments is too low to find the proper heat treatment parameters, e.g. carbon potential, tapping temperature, quenching temperature, and holding times for tempering. With the rapid development of computation techniques, numerical modeling has emerged as a powerful tool for the R&D of heat treatments of metallic materials [7-9].

In the present work, a rapid carburization technique for a 18Cr2Ni4WA alloy steel is proposed through the experimental study together with numerical modeling. The microstructure of the effective hardening layer and the interior area of the heavy-duty gears is observed, and the effects of strengthening of the hardening layer are characterized through the distribution of Vickers hardness. The finite-element-method (FEM) modeling of the carburization heat treatment is performed, in which the evolution of the phase fractions of austenite, martensite, and bainite is obtained. The hardness distribution is calculated according to the Maynier equation [10]. The data of hardness obtained from experiments and FEM modeling are compared for detailed analyses.

2. Experimental and Numerical Modeling

The schematic sketch of the carburization heat treatment is illustrated in figure 1. It can be seen that there are six steps, i.e. carburization, high-temperature tempering twice, quenching, cold treatment, and low-temperature tempering. The carburizing temperature is 970 ℃, which is 50 ℃ higher than the previous technique. The values of the carbon contents in the carburizing and diffusion stages are 1.3 wt.% and 0.85 wt.%, respectively. The high-temperature tempering processes are carried out twice after the carburization, and followed by an oil quenching process. Cold treatment at the temperature of -70 ℃ is performed for 2 hours to reduce the fraction of the residue austenite. The final heat treatment is the low-temperature tempering for reducing the internal stress caused by the quenching and the -70 ℃ cold treatment. The cylindrical specimens with a 40 mm diameter are used. The chemical compositions of the specimens (18Cr2Ni4WA) are listed in table 1.

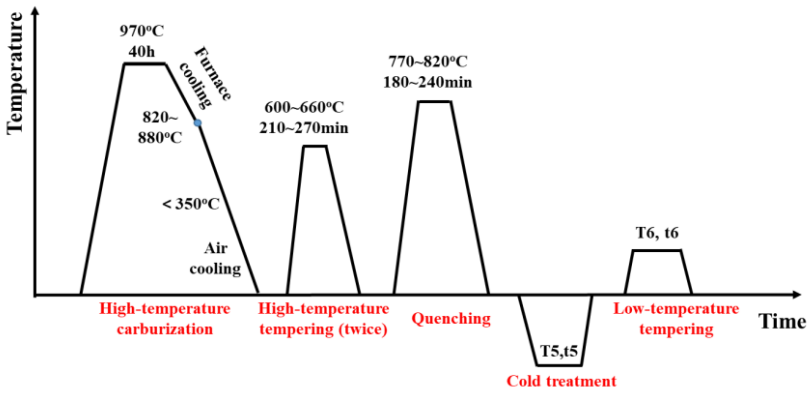

Figure 1. Sketch of the carburization heat treatment for a 18Cr2Ni4WA alloy steel.

Table 1. Chemical composition of the 18Cr2Ni4WA steel specimens (weight percent, wt. %).

C	Cr	Ni	W	Mn	Si	Fe
0.14	1.45	4.14	0.79	0.46	0.24	Bal.

After each step of the heat treatments, the samples for microstructure observation were taken in the hardening layer (2 mm from the surface) and the interior area (center) of the cylindrical specimens. The microstructure is observed by using scanning electron microscopy (SEM, ZEISS GeminiSEM 300). The Vickers hardness distribution is measured by using the tester produced by Shanghai Hengyi Corporation (MH-500).

The FEM modeling of the carburization heat treatment is performed by using the software DEFORM. The 18Cr2Ni4WA steel corresponds to 655M13 in the material database. The size of the cylindrical specimen in the FEM simulation is identical to the carburizing experiment. The Maynier equation for the computation of the Vickers hardness is [10]

$$HV = \xi_M \cdot HV_M + \xi_B \cdot HV_B + \xi_A \cdot HV_A \tag{1}$$

where ξ_M, ξ_B, and ξ_A are the calculated phase fractions of martensite, bainite, and residue austenite, respectively. HV_M, HV_B, and HB_A are the Vickers hardness of the pure microstructure of martensite, bainite, and residue austenite, respectively. In this work, HV_M, HV_B, and HB_A are calculated by [10]

$$HV_M = 127 + 949\mathrm{C} + 27\mathrm{Si} + 11\mathrm{Mn} + 8\mathrm{Ni} + 16\mathrm{Cr} + 21\lg V_r \tag{2}$$

$$\begin{aligned} HV_B = {} & 323 + 185\mathrm{C} + 330\mathrm{Si} + 153\mathrm{Mn} + 65\mathrm{Ni} + 144\mathrm{Cr} + 191\mathrm{Mo} \\ & + (89 + 53\mathrm{C} - 55\mathrm{Si} - 22\mathrm{Mn} - 10\mathrm{Ni} - 20\mathrm{Cr} - 33\mathrm{Mo})\lg V_r \end{aligned} \tag{3}$$

where V_r is the cooling rate that is calculated from the FEM modeling. The physical symbols of the elements, e.g. C, Si, and Mn, are the corresponding weight percent. It can be seen that the HV_M and HV_B are positively dependent on the weight percent of carbon.

Thus, it is expected that the values of HV_M and HV_B in the hardening layer with high carbon concentrations are higher than those in the interior area. Since the carbon concentration gradually decreases from the hardening layer to the interior area, the values of HV_M and HV_B should also present decreasing trends. In addition, it should be noted that in the present work the austenite hardness, HV_A in Eq. (1), is set to be 240.

3. Results and Discussion

3.1. FEM Simulation

Figure 2 illustrates the calculated distribution of carbon concentration after the high-temperature carburization. After 40 hours of carburization, the final distribution of the carbon concentration presents a decreasing trend from the surface to the interior area. The carbon atoms cannot reach the interior area of the cylindrical specimen, so that the carbon concentration becomes stable. The maximum carbon concentration appears on the surface of the specimen, which equals the carbon content in the diffusion stage. It can be seen that the thickness of the hardening layer is about 4 mm.

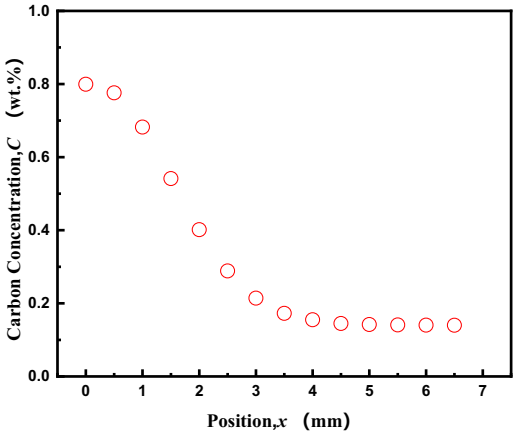

Figure 2. Carbon concentration distribution after carburization obtained from the FEM simulation.

Figure 3 shows the calculated results of the fractions of martensite, bainite, and austenite after the low-temperature tempering, as well as the comparison of hardness distributions obtained from experiments and FEM simulation. As shown in figure 3(a), the primary microstructure in the hardening layer is martensite, and the fractions of bainite and residue austenite are minor. In the interior area of the specimen, it is seen that the bainite fraction is higher, since the cooling rate in the interior area is lower than that in the hardening layer. On the other hand, it is observed that the residue austenite only exists in the hardening layer, i.e. in the region having a high carbon concentration. This is because the high carbon concentration is beneficial for the austenite remaining. In figure 3(b), the calculated data of the hardness are obtained from Eq. (1). As expected, the calculated hardness profile presents a decreasing trend from the surface to the interior

of the specimen. For the experimentally measured data, however, the hardness increases before it decreases. The relatively lower hardness at the surface is because of the decarburization effect when the specimen is taken out from the furnace at an elevated temperature. Nevertheless, it is observed that the measured hardness values are close to the FEM calculated results. The agreements of the hardness data obtained from the experiments and numerical simulation demonstrate the feasibility of using FEM simulation to partly replace the trial-and-error experiments for increasing the R&D efficiency.

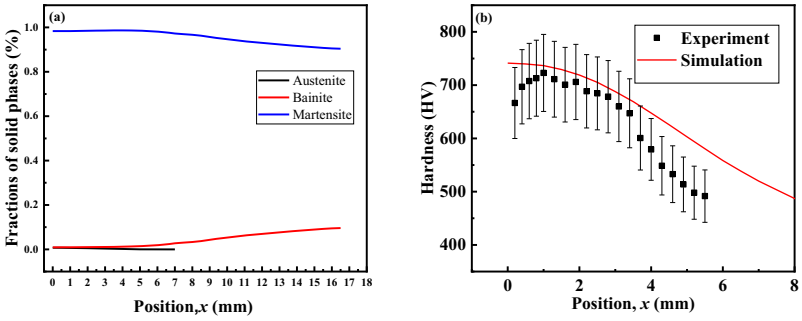

Figure 3. (a) Simulation results of phase fractions of martensite, bainite, and austenite after the low-temperature tempering; (b) Comparison of Vickers hardness distributions obtained from experiments and FEM simulation.

3.2. Microstructure Observation of the Hardening Layer and the Interior Area

Figure 4 exhibits the photographs of the microstructure in the hardening layer after each step of heat treatment. It can be seen in figure 4(a) that microstructure is mainly high-carbon martensite, since the quenching degree of the steel is high. After twice of high-temperature tempering, the tempered martensite microstructure is observed, see figures 4(b) and (c), and some small carbides are seen due to the partial decomposition of austenite. The martensite and carbide particles are observed after quenching (figure 4(d)). The cold treatment is set for decreasing the fraction of the residue austenite. As compared in figures 4(d) and (e), however, the microstructure has little change after the cold treatment. After the low-temperature tempering that is for reducing the internal stress, see figure 4(f), the carbides are more obvious. From the view of the microstructure in figures 4(d)-(f), the mechanical property should be similar. The hardness of the hardening layer is high due to the combination of martensite and the high density of carbide particles.

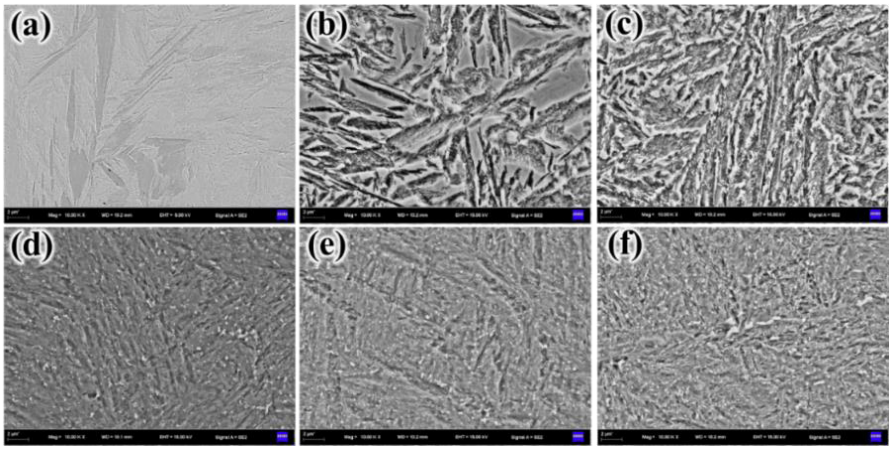

Figure 4. SEM photographs of the microstructure in the hardening layer after (a) high-temperature carburization, (b) first high-temperature tempering, (c) second high-temperature tempering, (d) quenching, (e) cold treatment, and (f) low-temperature tempering.

The mechanical property of the interior area is significant for the toughness of the heavy-duty gears. Figure 5 displays the microstructure of the interior area. It can be seen in figure 5(a) that low-carbon martensite is the main microstructure. After the high-temperature tempering processes, there are no carbides in the microstructure (see figures 5(b) and (c)), since the carbon content is low. After quenching, as shown in figure 5(d), fine low-carbon martensite is obtained. Similar to the microstructure in the hardening layer, the martensite microstructure has little variation after the cold treatment and low-temperature tempering, see figures 5(e) and (f).

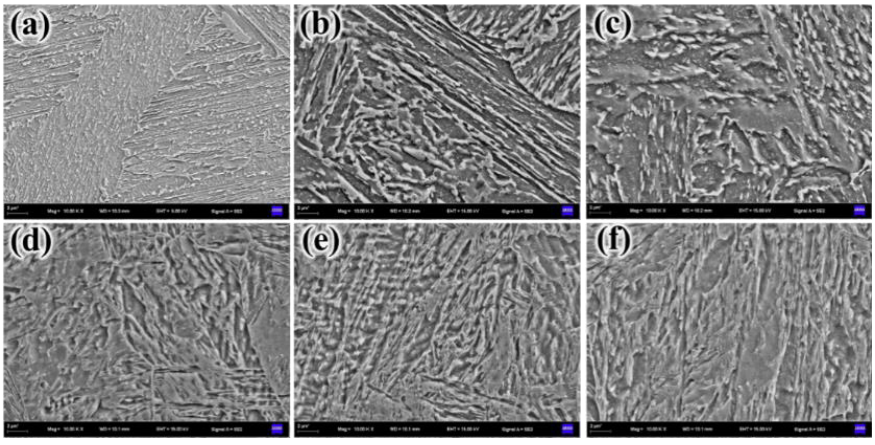

Figure 5. SEM photographs of the microstructure in the interior area after (a) high-temperature carburization, (b) first high-temperature tempering, (c) second high-temperature tempering, (d) quenching, (e) cold treatment, and (f) low-temperature tempering.

Figure 6 exhibits the former austenite grains in the hardening layer and interior area of the specimens after the steps of carburization and quenching. The blue lines are drawn according to the former grain boundaries. It is calculated that the grain size in the hardening layer after carburization is about 104.9 μm, while it becomes 51.8 μm after

quenching. The grains in the interior area also become finer by the tempering and quenching. Namely, the grain size evolves from 65.1 μm to 30.5 μm. The experimental observation indicates that the effects of the twice high-temperature tempering and quenching on grain refinement are remarkable.

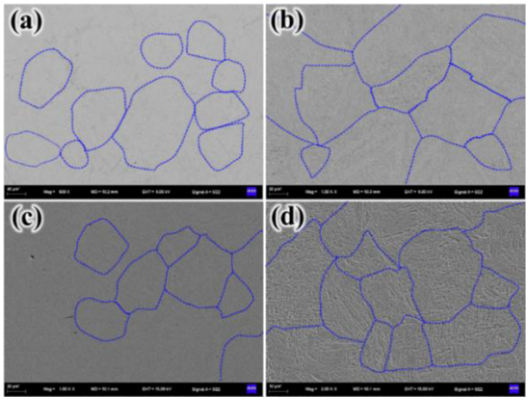

Figure 6. SEM photographs of the microstructure in the hardening layer and interior area after the carburization and quenching: (a) carburization, hardening layer; (b) carburization, interior area; (c) quenching, hardening layer; (d) quenching, interior area.

4. Conclusions

In this study, the rapid carburization process and the subsequent heat treatment of a 18Cr2Ni4WA alloy steel are studied through experiments and numerical modeling. The carbon concentration distribution after carburization is obtained from the FEM modeling. The phase fractions of austenite, bainite, and martensite are calculated, and the hardness distribution from the hardening layer to the interior area is computed according to the Maynier equation. The computed hardness compares well with the experimental data, demonstrating the validity of the FEM model. The microstructure after each step of heat treatment is observed by using SEM. The final microstructure in the hardening layer is fine martensite and carbides. The final microstructure in the interior area is the martensite. After the twice high-temperature tempering and quenching processes, the grains in the hardening layer and the interior area become finer. Through the combination of numerical modeling and experiments, the R&D efficiency of rapid carburization and the subsequent heat treatment becomes higher. The technique of numerical modeling could not only replace a part of trial-and-error experiments, but also guide the improvement of parameters in different steps of carburization heat treatments.

Acknowledgments

The authors thank the technicians in Yangtze Delta Region Institute of Advanced Materials for the SEM experiments.

References

[1] Fu HF, Li Q, Xu YM. Heat treatment technologies and its application of heavy-duty gears. Heat Treatment of Metals. 2020; 45: 178-185.
[2] Feng D, Kang BW, Shi L, Peng TF, Xiang ZX. Analysis of contact strength of large module heavy load rack and pinion, China Petroleum Machinery. 2018; 46: 14-19.
[3] Yuan YD. Analysis on cracking failure of 18Cr2Ni4WA large gear. Metal Processing (Hot Working). 2019; 10: 6-8.
[4] Li BK, Lu JS. Experimental study on deep carburizing process and distortion control of large modulus rack. Journal of Mechanical Transmission. 2020; 44: 160-163
[5] Zhou XH, Zhu K. Effects of cryogenic treatment on microtructure and properties of 18Cr2Ni4WA carburizing and quenching. Hot Working Technology. 2020; 49:147-149.
[6] Li GJ, Chen DH, Ren SZ, Ha SN, Liu GY, Wang H. Discuss of deep carburizing lean process for heavy-duty large module gear. Heat Treatment Technology and Equipment. 2013; 34:31-36.
[7] Sinha VK, Prasad RS, Mandal A, Maity J. A mathematical model to predict microstructure of heat-treated steel. Journal of Materials Engineering and Performance. 2007; 16: 461-469.
[8] Zhang QY, Sun DK, Pan SY, Zhu MF. Microporosity formation and dendrite growth during solidification of aluminum alloys: Modeling and experiment. International Journal of Heat and Mass Transfer. 2020; 146: 118838.
[9] Romedenne M, Rouillard F, Monceau D. Carburization of austenitic and ferritic stainless steels in liquid sodium: Comparison between experimental observations and simulations. Corrosion Science. 2019; 159: 108147.
[10] Bagali SV, Maruti NR, Abhaya S, Sushanth MP, et al. Estimation of hardness during heat treatment of EN8 and C25 Steels. in: K. Shanker, R. Shankar, R. Sindhwani (Eds.) Advances in Industrial and Production Engineering, Springer Singapore, Singapore. 2019; p. 149-160.